Desalination and Water Treatment
www.deswater.com

doi: 10.1080/19443994.2013.833875

52 (2014) 7887–7897
December

Taylor & Francis
Taylor & Francis Group

Kinetics and equilibrium adsorption of iron (II), lead (II), and copper (II) onto activated carbon prepared from olive stone waste

Tamer M. Alslaibi[a], Ismail Abustan[a,*], Mohd Azmier Ahmad[b], Ahmad Abu Foul[c]

[a]*School of Civil Engineering, Engineering Campus, Universiti Sains Malaysia, Nibong Tebal 14300, Pulau Pinang, Malaysia*
Tel. +6 04 5996259; Fax: +6 04 5941009; email: ceismail@eng.usm.my
[b]*School of Chemical Engineering, Engineering Campus, Universiti Sains Malaysia, Nibong Tebal 14300, Pulau Pinang, Malaysia*
[c]*Environmental Engineering, Islamic University of Gaza, Gaza, Palestine*

Received 1 May 2013; Accepted 15 July 2013

ABSTRACT

The adsorption of heavy metals Fe^{2+}, Pb^{2+}, and Cu^{2+} onto olive stone activated carbon (OSAC) was investigated in this study. The effects of different reaction parameters (i.e. adsorbent dosage, contact time, shaking speed, and initial pH) on the pollutant removal efficiency were determined. The adsorption processes of Fe^{2+}, Pb^{2+}, and Cu^{2+} were effectively explained using Langmuir and Freundlich isotherms. OSAC efficiently removed 99.39% Fe^{2+}, 99.32% Pb^{2+}, and 99.24% Cu^{2+} at pH 5 and with 200 rpm shaking speed. The adsorption equilibrium data were best represented by the Langmuir model, and the monolayer adsorption capacities were found to be 57.47, 22.37, and 17.83 mg/g for Fe^{2+}, Pb^{2+}, and Cu^{2+}, respectively. A pseudo-second-order model sufficiently described the adsorption kinetics, which indicated that the adsorption process was controlled by chemisorption. The results revealed that OSAC can be used as a low-cost adsorbent for the treatment of wastewaters contaminated by heavy metals.

Keywords: Olive stone; Activated carbon; Adsorption; Isotherm; Heavy metals; Kinetics

1. Introduction

The presence of heavy metals in aquatic environments has been of great concern because of their increased discharge, toxic nature, and other adverse effects on receiving waters [1]. Regarding environmental compartments, heavy metals show an ecological and human health issue because heavy metals do not undergo biological degradation unlike certain organic pollutants [2,3]. Accordingly, the safe and effective disposal of wastewater containing heavy metals is always a challenge to industrialists and environmentalists because cost-effective treatment alternatives are not available. Iron (Fe^{2+}), lead (Pb^{2+}), and copper (Cu^{2+}) have been introduced into natural waters from various sources, such as wastewater discharged from hospitals [4] and different industries, including smelting, metal plating, Cd–Ni battery, alloy manufacturing, phosphate fertilizer, mining pigment, and stabilizer production [5].

Physical and chemical treatment processes, such as coagulation, flotation, chemical precipitation,

*Corresponding author.

membrane filtration, and electrochemical methods, are used to remove heavy metals from wastewater [6]. However, these methods have lack of significance mainly due to their high capital and operational cost, disposal of residual metal sludge, continuous need of chemicals, and, sometimes, failure to meet acceptable limits of environmental protection agencies [7]. Therefore, there is a pressing need for more cost-effective and environmentally friendly methods. One of the most commonly used techniques involves the process of adsorption, which is the adhesion of chemicals onto a solid surface [8].

The use of adsorbents, such as rice husks [9], polygonum orientale [10], mangosteen shell [11], pomegranate peel [12], and sawdust [13] for the removal of dyes or single metal of Fe^{2+}, Pb^{2+}, or Cu^{2+} from aqueous solution has been reported.

However, studies on metal removal using olive oil solid residues are still limited. Thus, this study aims to evaluate the effectiveness of olive stone activated carbon (OSAC) for removing a group of metals in a model aqueous solution namely, Fe^{2+}, Pb^{2+}, and Cu^{2+}. Olive stone (OS) waste residue as a raw material for the production of activated carbon (AC) can be considered as one of the best candidates among agricultural waste because it is cheap and quite abundant, especially in Mediterranean countries. To investigate the process variables, including dosage, contact time, shaking speed, and initial pH, suitable isotherm models and kinetics coefficients of OSAC for the removal of Fe^{2+}, Pb^{2+}, and Cu^{2+} were used.

2. Material and methods

2.1. Aqueous solution

Approximately, 1,000 mg/L stock solution was prepared by dissolving appropriate amounts of $FeSO_4.7H_2O(s)$, $Pb(NO_3)_2(s)$, and $CuCl_2.2H_2O(s)$ in deionized water. Then, 20 mg/L test solutions of Fe^{2+}, Pb^{2+}, and Cu^{2+} were prepared by successively diluting the stock solution. Metal standard solutions of 1,000 mg/L also purchased from Merck were used for inductively coupled plasma (ICP)-optical emission spectroscopy (VARIAN 715-ES).

2.2. Preparation and characterization of OSAC

OS waste was obtained from Gaza, Palestine. The OS waste was rinsed thrice with hot water, thrice with cold water, and dried in an oven at 105°C for 24 h to remove moisture content. Once dried, they were ground and sieved for a particle size of 2.0–4.75 mm [14] and loaded in a stainless steel vertical tubular reactor placed in a tube furnace. Carbonization step was carried out at 600°C for 1 h under purified nitrogen (99.99%). The char was mixed with KOH pellets at ratio of 1:1.25. Deionized water was then added to dissolve all the KOH pellets. Impregnation was performed for 24 h at room temperature, thus incorporating all the chemicals into the core of the particles. The activation step was conducted at 600°C for 2 h under a nitrogen flow of 150 cm^3/min at a heating rate of 10°C/min in a muffle furnace for the optimization of the reaction parameters. However, for the isotherm and kinetics examination, a temperature of 715°C, activation time of 2 h, and chemical impregnation ratio (char: KOH) of 1: 1.53 were used. These preparation conditions were selected based on optimization elsewhere [15]. The sample was then cooled to room temperature under nitrogen flow and washed with hot deionized water and 0.1 M HCl until the pH of the washed solution was within the range 6.5–7.

2.3. BET, SEM, and FTIR of the prepared OSAC

The surface area, pore volume, and average pore diameter of the OSAC were determined using a Micromeritics ASAP 2020 volumetric adsorption analyzer. The BET surface area was measured from the adsorption isotherm using the BET equation. The total pore volume was estimated as the liquid volume of nitrogen at a relative pressure of 0.98. The surface morphology of the samples was examined using a SEM system (Quanta 450 FEG, the Netherlands). The proximate analysis was performed using a thermo gravimetric analyzer (Perkin–Elmer TGA7, USA). Chemical characteristics of surface functional groups of the AC were detected by diluting in K-Br pellets were recorded with FTIR spectroscope (IR Prestige 21 Shimadzu, Japan) in the 400–4,000 cm^{-1} wave number range.

2.4. Batch equilibrium studies

Batch equilibrium tests were conducted to study Fe^{2+}, Pb^{2+}, and Cu^{2+} adsorption on OSAC. The effects of adsorbent dosage, contact time, shaking speed, and initial pH on the adsorption uptake were investigated. Optimization of the media performance was achieved by monitoring the influence of each factor, one at a time, on experimental responses. This optimization is called the one-variable-at-a-time method, in which only one variable is varied while the others are maintained at a constant level [16,17].

The effect of the adsorbent dose on Fe^{2+}, Pb^{2+}, and Cu^{2+} removal was studied by agitating 100 mL of 20 mg/L solution of Fe^{2+}, Pb^{2+}, and Cu^{2+} containing

different doses of adsorbent (0.025–2.0 g) for 3 h using an orbital shaker (Lab. Companion, Model SK-600). The effect of different contact times on Fe^{2+}, Pb^{2+}, and Cu^{2+} removal was studied using 100 mL of 20 mg/L solutions of Fe^{2+}, Pb^{2+}, and Cu^{2+} agitated with 0.3 g of adsorbent for different contact times (0.1–24 h). The rate of removal of Fe^{2+}, Pb^{2+}, and Cu^{2+} at different shaking speed values (50–300 rpm) was studied by agitating 100 mL of 20 mg/L of Fe^{2+}, Pb^{2+} and Cu^{2+} solutions with 0.3 g of adsorbent for 3 h. The effect of pH on Fe^{2+}, Pb^{2+}, and Cu^{2+} removal was studied using 100 mL of 20 mg/L solutions of Fe^{2+}, Pb^{2+}, and Cu^{2+} adjusted to initial pH 2 to pH 6 and agitated with 0.3 g of adsorbent for 3 h. This pH range was selected to avoid metal solid hydroxide precipitation. In the case of the metals under study, metal hydroxide precipitation occurs at pH > 6.0 for Cu(II) and Pb (II) [18] and at pH > 8 for $Fe(OH)_2$(s) [19]. All pH measurements were conducted using a pH meter (Witeng, W-100, Germany). The initial pH levels of the experimental solutions were adjusted using 0.1 M solution of HCI or NaOH.

After agitation, the solid was removed by filtration through a 0.45 μm pore size Whatman membrane filter paper. The final metal concentration in the filtrate as well as in the initial solution was determined using an ICP optical emission spectroscopy system (Varian, 715-ES). The sorbed metal concentrations were obtained from the difference between the initial and final metal concentrations in solution. The amount of adsorption at equilibrium q_e (mg/g) was calculated using Eq. (1):

$$q_e = \frac{(C_0 - C_e)V}{W} \quad (1)$$

where C_0 and C_e (mg/L) are the liquid-phase concentrations of Fe^{2+}, Pb^{2+}, and Cu^{2+} at the initial and equilibrium states, respectively; V (L) is the volume of solution; and W (g) is the mass of dry adsorbent used.

The percentage removal at equilibrium was calculated using Eq. (2):

$$\text{Removal}\,(\%) = \frac{C_0 - C_e}{C_0} \times 100 \quad (2)$$

where, C_0 and C_e (mg/L) are the liquid-phase concentrations of Fe^{2+}, Pb^{2+}, and Cu^{2+} at the initial and equilibrium states, respectively.

2.5. Batch kinetic studies

The procedure for the kinetic adsorption tests was identical to that of the batch equilibrium tests. However, the aqueous samples were obtained at selected time intervals. The concentrations of Fe^{2+}, Pb^{2+}, and Cu^{2+} were simultaneously determined. The Fe^{2+}, Pb^{2+}, and Cu^{2+} uptake at any time, q_t (mg/g), was calculated by:

$$q_t = \frac{(C_0 - C_t)V}{W} \quad (3)$$

where C_t (mg/L) is the liquid-phase concentration of Fe^{2+}, Pb^{2+}, and Cu^{2+} at any time, t (h).

3. Results and discussion

3.1. Characterization of OSAC

Among the most important features of adsorbents are their surface area and porosity. The BET surface area, mesopore surface area, total pore volume, and average pore diameter of the prepared AC were 886.72 m^2/g, 740.66 m^2/g, 0.507 cm^3/g, and 4.92 nm, respectively. The average pore diameter of 4.92 nm indicated that the OSAC was in the mesoporous region [20]. The high surface area and pore volume of the OSAC were due to the activation process used that involved KOH. The proximate values of the OS raw and OSAC are presented in Table 1. After the activation process, the volatile matter content decreased significantly, whereas the fixed carbon content increased in OSAC. This resulted from the pyrolytic effect, by which most of the organic substances are degraded and discharged as gas and liquid tars leaving a material with high carbon purity [21].

Fig. 1(a) and (b) show the SEM images of the OS raw and the derived OSAC, respectively. Large and well-developed pores were obviously formed on the surface of the OSAC compared with the OS raw. KOH and the activation process are effective in forming well-developed pores on the OSAC surfaces, leading to AC with large surface area and good porous structure (mesoporous). Almost all heterogeneous types of pore structure were also distributed on the OSAC surface. Several authors found similar observa-

Table 1
Proximate analysis

Sample	Proximate analysis (%)			
	Moisture	Volatile	Fixed carbon	Ash
OS raw	8.70	65.31	18.53	7.46
OSAC	4.20	20.35	71.17	4.28

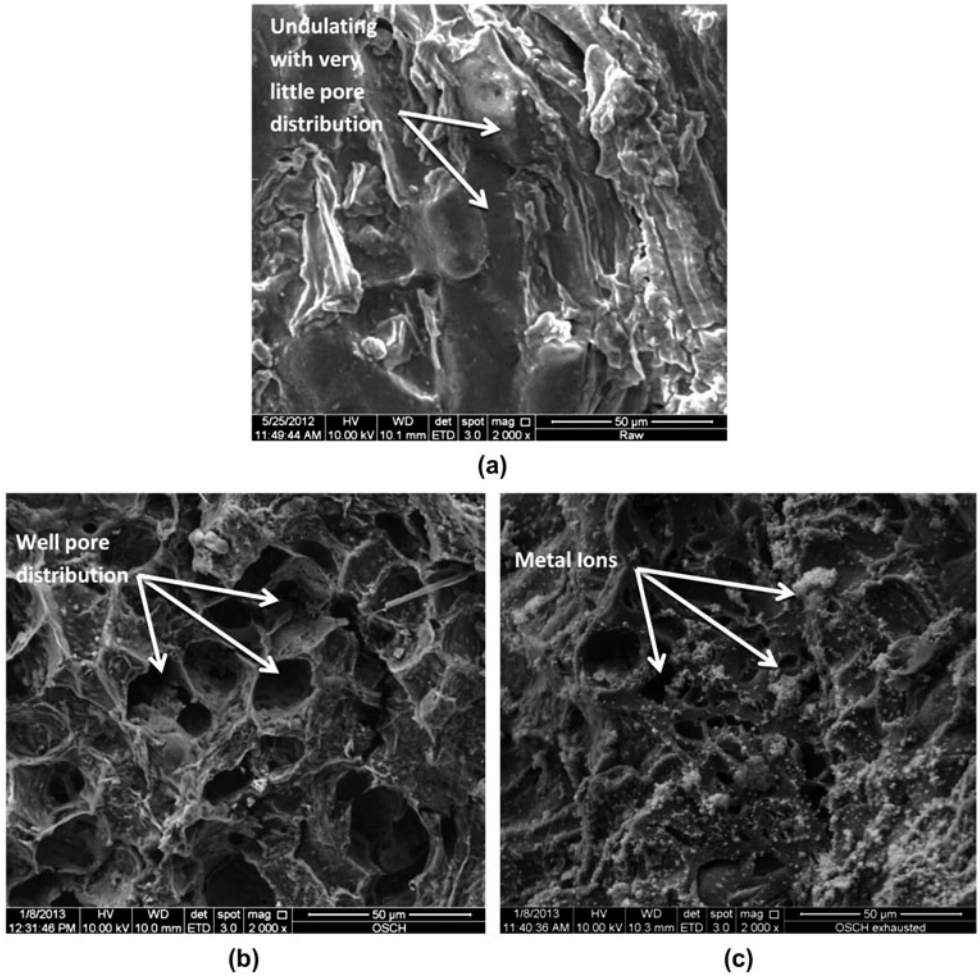

Fig. 1. SEM: (a) OS raw (b) OSAC before adsorption (C) after adsorption (magnifications: 2000×).

tions in their studies on preparing AC from walnut shells [22], jute and coconut fibers [23], and bamboo waste [24].

The obtained FTIR spectrum of OS raw (Fig. 2(a)) revealed the peaks at 3,857, 2,295, 1,739, 1,527, and 1,018 cm^{-1}, corresponds to the presence of –OH (hydroxyl), C≡C (alkynes), –COOH (carboxylic acids), in-plane –OH, and C–O–C (esters, ether, or phenol) functional groups. Meanwhile, the surface chemistry of OSAC (Fig. 2(b)) revealed the region between 3,861 and 3,587 cm^{-1}, corresponds to the presence of–OH (hydroxyl) functional groups, and the broad band at 2,287–2098 cm^{-1} is assigned to the –COOH and C≡C derivatives. The sharp peak at 995 cm^{-1} is ascribed to the C–H stretching in alkanes group, and the signal at 590 cm^{-1} is associated with the C≡C stretching of alkyne group and C–H stretching in alkanes group. Other major peaks also detected at bandwidths 1905, 1,729, and 1,531 cm^{-1} assigned to C=O stretching of aldehydes and ketones group, and the vibration of C=C stretching of aromatic group, respectively. The surface chemistry of OS raw and OSAC found to be different as some of the functional groups were disappeared due to the activation process. Based on experimental results and the speciation of metal ions, metal removal by OSAC may have occurred through the complexation between the negatively charged functional groups, such as carboxylic groups (–COOH) and hydroxyl groups (–OH) [25], and metal cations Me^{+2}. At pH higher than 3 to 5, carboxylic groups are deprotonated and negatively charged. Accordingly, the attraction of positively charged metal ions would be improved. In other words, the adsorptive characteristic was influenced by the surface functionalities, which may serve as the chemical binding sites for the adsorption process. Besides, the presence of hydroxyl, carbonyl, and alkyl groups could dissociate as negatively charge sites, and contributing to electrostatic

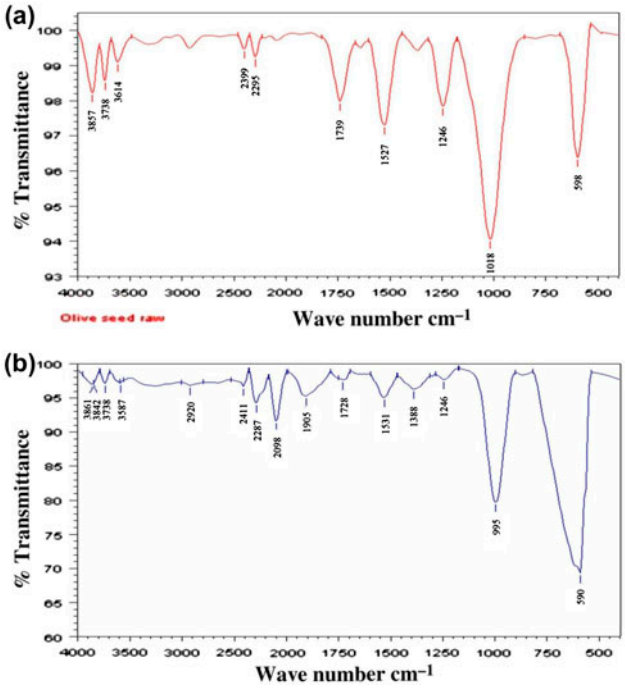

Fig. 2. FTIR of (a) OS raw and (b) OSAC.

attraction between the ACs and the positively charged metal ions [26].

3.2. Effect of adsorbent dosage

The adsorbent OSAC dosage is an important parameter for analyzing the quantitative uptake of pollutants. Pollutant retention was examined in relation to the amount of adsorbent. The results of the removal of Fe^{2+}, Pb^{2+}, and Cu^{2+} using OSAC are shown in Fig. 3. The shaking speed, contact time, and initial pH level were 200 rpm, 3 h, and 4.5, respectively. The dosage of the OSAC adsorbent varied from 0.025 to 2 g. The percentage of pollutant removal increased with increasing dosages of the OSAC, after which it became constant. The best results were obtained using a dosage of 0.3 g, where 99.77% Fe^{2+}, 99.24% Pb^{2+}, and 99.08% Cu^{2+} were removed. This was because the number of available adsorption sites increased through the increase in adsorbent dose [12, 27]. A dosage greater than 0.3 g led to a nonsignificant increase in Fe^{2+}, Pb^{2+}, and Cu^{2+} removal. Thus, a dosage of 0.3 g of OSAC was selected for all subsequent experiments.

3.3. Effect of contact time

Fig. 4 shows the effect of contact time on Fe^{2+}, Pb^{2+}, and Cu^{2+} uptakes. The contact time for the OSAC (dosage of 0.3 g; solution volume of 100 mL; shaking speed of 200 rpm; initial pH of 4.5) varied from 0.1 h to 24 h. It was observed that the Fe^{2+}, Pb^{2+}, and Cu^{2+} adsorption was fast during the initial 20 min, after which it became slower until it reached a constant value after 3 h where no more metals can be removed from the solution. The rapid metal adsorption was caused by the large number of surface sites available for adsorption at the initial stage. As the reaction proceeds, the remaining surface sites become difficult to occupy because of the repulsion between the solute molecules of the solid and bulk phases [28]. Thus, for all the subsequent experiments, a contact time of 3 h was selected.

3.4. Effect of shaking speed

The effect of shaking speed on Fe^{2+}, Pb^{2+}, and Cu^{2+} removal are demonstrated in Fig. 5. The effects were studied using 0.3 g of OSAC with a contact time of 3 h and different shaking speeds (50–350 rpm). The results indicated that the removal of the metals

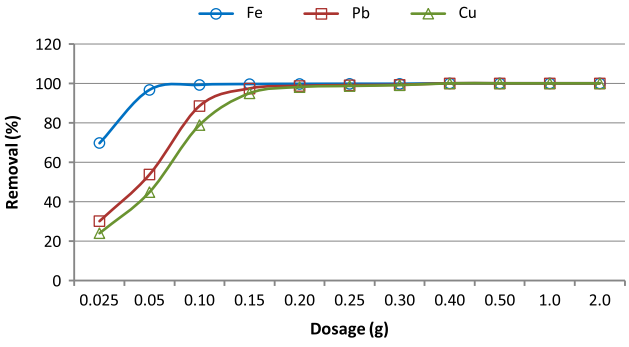

Fig. 3. Effect of OSAC dosages on Fe^{2+}, Pb^{2+}, and Cu^{2+} removal by OSAC.

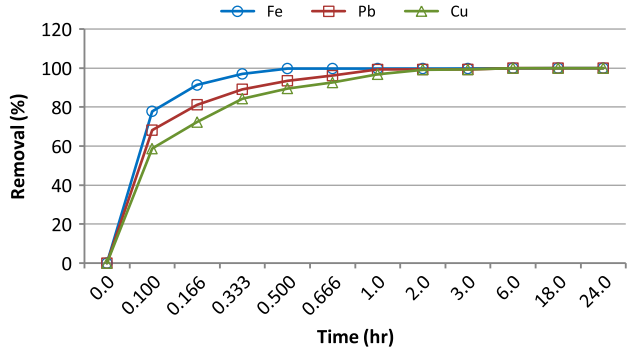

Fig. 4. Effect of contact time on Fe^{2+}, Pb^{2+}, and Cu^{2+} removal by OSAC.

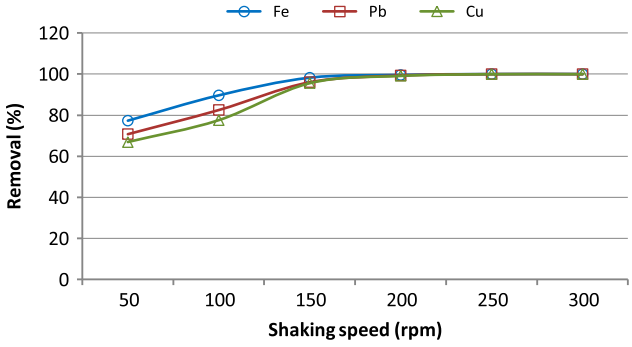

Fig. 5. Effect of shaking speed on Fe^{2+}, Pb^{2+}, and Cu^{2+} removal by OSAC.

increased as the shaking speed increased up to 200 rpm; at higher speeds, the removal rate remained constant. According to Chabani et al. [29], the resistance of the boundary layer surrounding the adsorbate weakens at strong agitation rates. Thus, for all the subsequent experiments, a shaking speed of 200 rpm was selected.

3.5. Effect of solution pH

The removal of metal ions from aqueous solution by adsorption is highly dependent on the pH of the solution, which affects the surface charge of the adsorbent and the degree of ionization and speciation of the adsorbate [30]. To verify the effect of pH on Fe^{2+}, Pb^{2+}, and Cu^{2+} removal using OSAC as adsorbent, experiments were conducted by modifying pH from 2 to 6 as shown in Fig 6. Initially, at low pH < 3, the minimal removal may be an effect of the higher concentration and high mobility of the H^+, which competes with metal ions on the active sites on the sorbent surface, resulting in its preferential adsorption rather than the metal ions [31]. Therefore, H^+ ions react with anionic

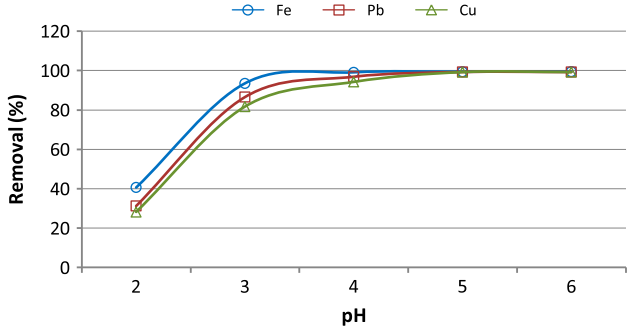

Fig. 6. Effect of solution pH on Fe^{2+}, Pb^{2+}, and Cu^{2+} removal by OSAC.

functional groups on the surface of OSAC and results in the reduction of the number of binding sites available for the adsorption of Fe^{2+}, Pb^{2+}, and Cu^{2+}. In Fig. 5, the percentages of Fe^{2+}, Pb^{2+}, and Cu^{2+} removal were found to increase significantly with the increase in solution pH from pH 3 to pH 6. The highest Fe^{2+}, Pb^{2+}, and Cu^{2+} removal of 99.39, 99.32, and 99.24%, respectively, were achieved at pH 5. This increase may have been an effect of the presence of negative charge on the surface of the adsorbent that may have been responsible for the metal binding because solution pH can affect the charge of OSAC surfaces [32]. In addition, at higher pH values, the lower number of H^+ and greater number of ligands with negative charges result in greater metal adsorption. In other words, monovalent cations, $Me(OH)^+$, are the dominant ion species at the optimal pH range. Based on experimental results and the speciation of metal ions, metal removal by OSAC may have occurred through the complexation between the negatively charged functional groups, such as carboxylic groups (–COOH) [25,33] and metal cations, such as Me^{+2} and $Me(OH)^+$. At pH higher than 3 to 4, carboxylic groups are deprotonated and negatively charged. Accordingly, the attraction of positively charged metal ions would be improved. Thereafter at pH 5–6, the metal removal remains almost constant. Thus, for all the subsequent experiments, an initial solution pH of 5 was selected to avoid metal hydroxide precipitation that occurs at pH > 6.0 for Cu (II) and Pb(II) [18] and at pH > 8 for $Fe(OH)_2(s)$ [19]. The same trend was observed by several researchers who studied metal sorption by different biomaterials, namely, iron by pine bark waste [34], copper by sawdust [35], and zinc, lead, and cadmium by jute fibers [36].

3.6. Adsorption isotherms

The Langmuir model is based on the assumption that adsorption energy is constant and independent of surface coverage. Maximum adsorption occurs once the surface is covered by a monolayer of adsorbate. The linear form of the Langmuir isotherm equation is given as:

$$\frac{1}{(q_e)} = \frac{1}{QbC_e} + \frac{1}{Q} \quad (4)$$

where C_e (mg/L) is the equilibrium liquid-phase concentration of metals, q_e (mg/g) is the equilibrium uptake capacity, Q (mg/g) is the Langmuir constant related to adsorption capacity, and b (L/mg) is the Langmuir constant related to the energy of sorption, which quantitatively reflects the affinity between the

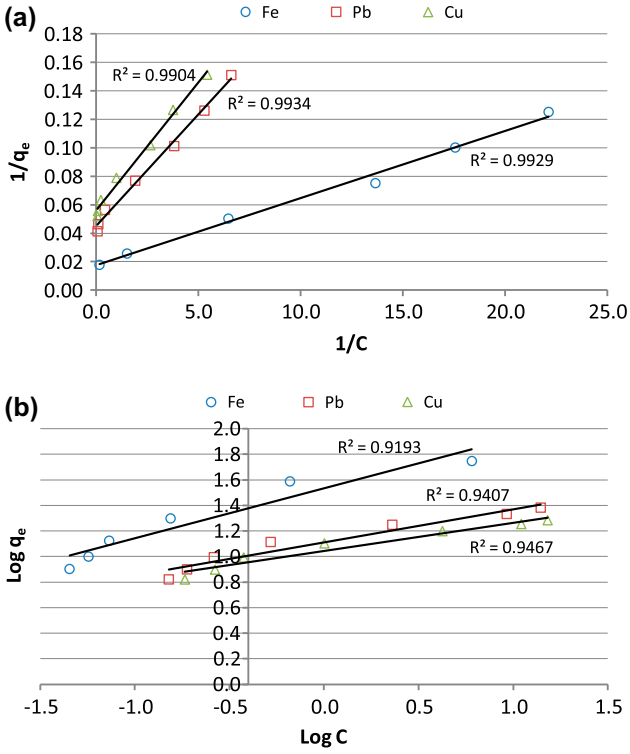

Fig. 7. Langmuir isotherm and Freundlich isotherm for Fe^{2+}, Pb^{2+}, and Cu^{2+} adsorption onto OSAC (contact time, 3 h; shaking speed, 200 rpm; initial pH, 5; initial concentration, 20 mg/L: (a) Langmuir isotherm and (b) Freundlich isotherm.

sorbent and the sorbate. A straight line was obtained when $1/(q_e)$ was plotted vs. $1/C_e$. Q was evaluated from the intercept, whereas b was determined from the slope Fig. 7(a). The equilibrium data were fitted to the Langmuir isotherm. The constants together with the coefficient of determination (R^2) values are listed in Table 2. As shown in Table 2, the highest value of adsorption capacity (Q) on the OSAC was found for Fe^{2+} (57.47 mg/g), followed by Pb^{2+} (22.37 mg/g) and Cu^{2+} (17.83 mg/g). Therefore, the adsorption capacity series, Fe > Pb > Cu, found in this study is in agreement with the first hydrolysis constant ($Me(OH)^+$) series, which is Fe > Pb > Cu [37]. However, the order of this series is slightly different from the relative affinity order of OSAC found on the basis of b values, which is Fe > Cu > Pb. This difference order may due to the presence of a further operating mechanism besides the basic ion-exchange, such as specific complexation by carboxylic and hydroxyl groups present in the basic fibrous cellulosic structure of this material [18].

The characteristics of the Langmuir isotherm can be expressed using the equilibrium parameter R_L:

$$R_L = \frac{1}{(1 + bC_0)} \tag{5}$$

where b is the Langmuir constant and C_0 is the initial pollutant concentration (mg/L). The value of R_L indicates whether the isotherm is unfavorable ($R_L > 1$), linear ($R_L = 1$), favorable ($0 < R_L < 1$), or irreversible ($R_L = 0$). The R_L values for the adsorption of Fe^{2+}, Pb^{2+}, and Cu^{2+} on the OSAC were 0.013, 0.017, and 0.016, respectively, indicating that the adsorption is a favorable process.

The Freundlich model is based on sorption on a heterogeneous surface of varied affinities. The linear form of Freundlich model is given as:

$$\log q_e = \log K + \frac{1}{n} \log C_e \tag{6}$$

where q_e (mg/g) is the amount of metals adsorbed at equilibrium, C_e (mg/L) is the adsorbate concentration, K_f (m/g)(L/mg)$^{1/n}$ is the Freundlich constant related to adsorption capacity, and $1/n$ is the Freundlich constant related to sorption intensity of the sorbent. Larger values of K_f mean greater capacities of adsorption [38].

The slope of $1/n$, ranging between 0 and 1, is a measure of the adsorption intensity or surface heterogeneity. This slope becomes more heterogeneous as its value approaches 0; $1/n < 1$ indicates a normal Freundlich isotherm, whereas $1/n > 1$ indicates cooperative adsorption [39]. The plot of log q_e vs. log C as shown in Fig. 7(b) gives a straight line with a slope of $1/n$. The value of K was calculated from the intercept value. The values of K, $1/n$, and R^2 for the Freundlich model are given in Table 2.

Table 2
Langmuir and Freundlich isotherm parameters for the adsorption of Fe^{2+}, Pb^{2+}, and Cu^{2+} onto OSAC

Parameter	Langmuir isotherm model				Freundlich isotherm model		
	Q (mg/g)	b (L/mg)	R^2	R_L	K (mg/g) (L/mg) $^{1/n}$	$1/n$	R^2
Fe	57.47	3.702	0.992	0.013	34.04	0.391	0.919
Pb	22.37	2.847	0.993	0.017	12.90	0.259	0.941
Cu	17.83	3.134	0.990	0.016	11.03	0.222	0.947

Table 3
Comparison of the biosorption capacity of different biosorbents

Sorbent	Preparation condition				Adsorption capacity (mg/g)					
	Modifying agent(s)	Temp. (°C)	Time (h)	IR	Fe	Pb	Cu	C_0	pH	Ref.
Cashew nut shells	KOH	850	2.5	4	–	28.9	–	40	6.0-6.5	[43]
Untreated coir fibres	–	–	–	–	2.84	–	–	74	5.0-6.6	[44]
Oxidised coir fibers	hydrogen peroxide and sodium hydroxide	85	2	–	7.49	–	–	74	5.0-6.0	[44]
Pine bark waste	Hydrogen peroxide	60	24	–	2.03	–	–	12-14	6.0-6.5	[45]
Untrated turkish fiy ashes	–	–	–	–	–	–	1.35	25	6.0	[46]
Untreated sphagnum moss peat	–	–	–	–	–	–	5.0	25	5.0	[47]
Pomegranate peel	H_3PO_4	500	1	1	–	5.6	5.8	50	5.6-5.8	[12]
Untreated mangosteen shell	–	–	–	–	–	–	3.15	50	5.0	[11]
Modified peanut husk	Formalin and H_2SO_4	50	3	–	–	29.14	10.15	50	4.0	[40]
Crosslinked chitosan	acetic acid	–	–	–	64.1	–	–	6.0	5.0	[19]
Jute fibres	Hydrogen peroxide and sodium hydroxide	85	2	4	–	–	4.23	75	5.0	[36]
Untreated petiolar felt-sheath of palm	–	–	–	–	–	11.4	8.09	100	5.0	[48]
Dye loaded groundnut shell	propanol-2	–	0.25	–	–	–	7.6	73	5.0	[49]
Olive stone	KOH	715	2	1.53	57. 47	22.37	17.83	20	5.0	This work

Note: IR: impregnation ratio.

The results indicate that the adsorption intensities were derived from the Freundlich coefficient, where the $1/n$ values of Fe^{2+}, Pb^{2+}, and Cu^{2+} at 0.391, 0.259, and 0.222, respectively, are less than one, which indicates a normal Freundlich isotherm. The adsorption of Fe^{2+}, Pb^{2+}, and Cu^{2+} was reasonably explained by the Langmuir and Freundlich isotherms. However, the Langmuir model yielded the best fit given that the R^2 values were relatively higher (close to unity). These results were confirmed by the high values of R^2 for Fe^{2+}, Pb^{2+}, and Cu^{2+} in the case of the Langmuir model, which were 0.992, 0.993, and 0.990, respectively, compared with those of the Freundlich model, which were 0.919, 0.941, and 0.947, respectively.

Although the Freundlich isotherm model showed lower values of R^2 for Fe^{2+}, Pb^{2+}, and Cu^{2+}, a trend similar to that of the series Fe > Pb > Cu of adsorption capacity and Freundlich empirical constants, k and $1/n$, were obtained for all metals (Table 2). Larger values of k mean greater capacities of adsorption [38]. Therefore, sorption capacity and sorption intensity of OSAC for the studied metal ions may be in the order Fe > Pb > Cu. The results obtained agreed with those of the study of Li et al. [40], in which the following order for the sorption of metals onto sawdust and modified peanut husk was reported: Pb > Cu > Cr. Another study by Brown et al. [41] examined peanut hull pellets and found a similar order of affinity: Pb > Zn > Cu > Cd. El-Ashtoukhy et al. [12] also reported the following order for cation chelation capacity with pomegranate peel: Pb > Cu. Spinti et al. [42] reported a similar order of affinity for immobilized biomass (peat) beads: Fe > Al > Cu > Cd, Zn.

Table 3 lists the comparison of Fe^{2+}, Pb^{2+}, and Cu^{2+} adsorption for various ACs. The results obtained in the present work were comparable with the works reported in the literature.

3.7. Adsorption kinetics

Adsorption kinetics is of great significance in evaluating the performance of a certain adsorbent and in gaining insight into the underlying mechanisms [50]. Hameed [51] reported that kinetic modeling is generally used to investigate the mechanism of adsorption and the potential rate-controlling processes, such as mass transfer and chemical reaction. In the present study, the modeling of the kinetics of the adsorption of Fe^{2+}, Pb^{2+}, and Cu^{2+} on OSAC was investigated using two common models, namely, pseudo-first-order and pseudo-second-order models. The pseudo-first-order model is illustrated as follows:

$$\log(q_e - q_t) = \log(q_e) - \frac{K_1 t}{2.303} \quad (7)$$

A pseudo-second-order model is described as follows:

$$\frac{t}{q_t} = \frac{1}{K_2 q_e^2} + \frac{t}{q_e} \quad (8)$$

where q_e and q_t (mg/g) are the amounts of adsorbate adsorbed at equilibrium and at any time, t (h), respectively, and k_1 (1/h) is the adsorption rate constant. The linear plot of log ($q_e - q_t$) vs. t provides a slope of k_1 and intercept of log q_e as shown in Fig. 8(a). The values of k_1 and R^2 obtained from the plots for adsorption of Fe^{2+}, Pb^{2+}, and Cu^{2+} on the adsorbent are reported in Table 4. The R^2 values obtained for the pseudo-first-order model were not high. Besides, the experimental q_e values did not agree with the calculated values obtained from the linear plots. This finding shows that the adsorption of Fe^{2+}, Pb^{2+}, and Cu^{2+} on the adsorbent does not follow a pseudo-first-order kinetic model.

In the linear plot of t/q_t vs. t, $1/q_e$ was the slope and $1/k_2 q_e^2$ was the intercept. Fig. 8(b) shows a good agreement between the experimental and the calculated q_e values. Based on Table 4, all R^2 values obtained from the pseudo-second-order model were close to unity, indicating that the adsorption of Fe^{2+}, Pb^{2+}, and Cu^{2+} on OSAC fitted well into this model. A similar result was reported for the adsorption of heavy metals from aqueous solution onto AC from agricultural waste [12,40].

Table 4
Pseudo-first-order and pseudo-second-order kinetic model parameters for the adsorption of Fe^{2+}, Pb^{2+}, and Cu^{2+} onto OSAC at 20 mg/L concentration

Parameter	$q_{e,\,exp}$ (mg/g)	Pseudo-first-order model			Pseudo-second-order model		
		K_1 (1/h)	$q_{e,\,cal}$ (mg/g)	R^2	K_2 (g/mg h)	$q_{e,\,cal}$ (mg/g)	R^2
Fe	6.652	5.068	3.931	0.789	37.151	6.698	0.999
Pb	6.623	2.216	3.630	0.729	32.229	6.658	0.999
Cu	6.616	2.431	2.610	0.738	20.427	6.671	0.999

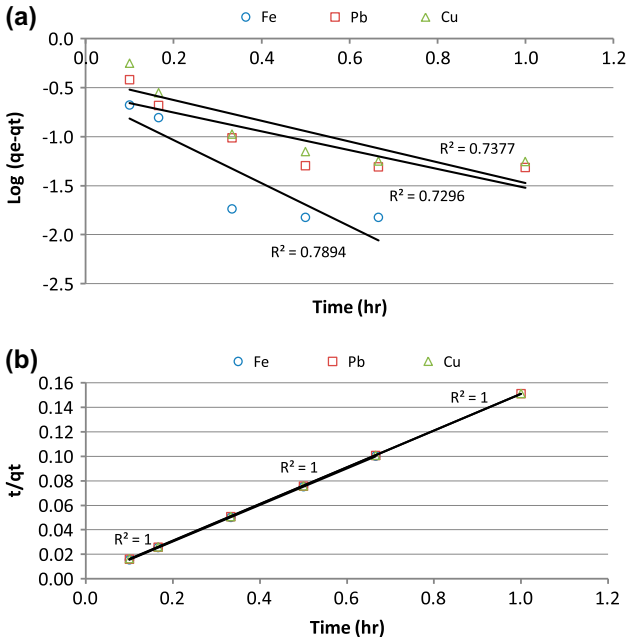

Fig. 8. Kinetic models for Fe^{2+}, Pb^{2+}, and Cu^{2+} adsorption onto OSAC (shaking speed, 200 rpm; initial pH, 5; initial concentration, 20 mg/L): (a) Pseudo-first-order kinetic model, and (b) Pseudo-second-order kinetic model.

3.8. OSAC power consumption

Power consumption estimates per kg of OSAC prepared via conventional thermal process were calculated based on the preparation condition. The carbonization step was carried out at 600°C for 1 h. The activation step for OSAC was at temperature 715° C and time 2 h. Carbonization step power consumption was 18.48 KWh/kg. For activation step, furans consumed 10.78 KW/h power for 0.5 kg OSAC, therefore activation step power consumption was 43.12 KWh/kg of OSAC. Thus, the calculated total power consumption of the preparation process was 61.60 KWh/kg of OSAC.

4. Conclusion

In the present study, the adsorption efficiency of Fe^{2+}, Pb^{2+}, and Cu^{2+} from aqueous solutions was investigated using OSAC. Metal adsorption was found to increase with an increase in OSAC dosage, contact time, and shaking speed. Solution pH > 5 was proven to be more favorable for adsorption of metals on OSAC. Experimental results showed that 99.39% of Fe^{2+}, 99.32% of Pb^{2+}, and 99.24% of Cu^{2+} were removed at pH 5. Adsorption equilibrium data were fitted to the Langmuir and Freundlich isotherm models and the kinetics data were fitted to the pseudo-second-order kinetics models. The results show that OS waste, which has an economic value, may be used for the treatment of wastewaters contaminated with heavy metals.

Acknowledgment

The authors wish to acknowledge the Universiti Sains Malaysia (USM) for its financial support under the USM and TWAS Fellowship scheme and acknowledge Ministry of Higher Education, Malaysia for providing LRGS grant no. (203/PKT/670006) and (03-01-05-SF0502) to conduct this study.

References

[1] M. Sekar, V. Sakthi, S. Rengaraj, Kinetics and equilibrium adsorption study of lead (II) onto activated carbon prepared from coconut shell, J. Colloid Interface Sci. 279 (2004) 307–313.
[2] E. Emmanuel, R. Angerville, O. Joseph, Y. Perrodin, Human health risk assessment of lead in drinking water: A case study from Port-au-Prince, Haiti, Int. J. Environ. Pollut. 31 (2007) 280–291.
[3] T.M. Alslaibi, I. Abustan, M.A. Ahmad, A. Abu Foul, Cadmium removal from aqueous solution using microwaved olive stone activated carbon, J. Environ. Chem. Eng. (2013). Available from http://dx.doi.org/10.1016/j.jece.2013.06.028.
[4] P. Verlicchi, A. Galletti, M. Petrovic, D. Barceló, Hospital effluents as a source of emerging pollutants: An overview of micropollutants and sustainable treatment options, J. Hydrol. 389 (2010) 416–428.
[5] I. Kula, M. Ugurlu, H. Karaoglu, A. Çelik, Adsorption of Cd (II) ions from aqueous solutions using activated carbon prepared from olive stone by $ZnCl_2$ activation, Bioresour. Technol. 99 (2008) 492–501.
[6] T.M. Alslaibi, I. Abustan, M.A. Ahmad, A. Abu Foul, Review: Comparison of agricultural by-products activated carbon production methods using surface area response, Caspian J. App. Sci. Res. 2 (2013) 18–27.
[7] R. Baccar, J. Bouzid, M. Feki, A. Montiel, Preparation of activated carbon from Tunisian olive-waste cakes and its application for adsorption of heavy metal ions, J. Hazard. Mater. 162 (2009) 1522–1529.
[8] T.M. Alslaibi, I. Abustan, M.A. Ahmad, A. Abu Foul, A review: Production of activated carbon from agricultural byproducts via conventional and microwave heating, J. Chem. Technol. Biotechnol. 88 (2013) 1183–1190.
[9] N. Yahaya, M. Latiff, I. Abustan, M.A. Ahmad, Effect of preparation conditions of activated carbon prepared from rice husk by $ZnCl_2$ activation for removal of Cu(II) from aqueous solution, Int. J. Eng. Technol. 10 (2010) 27–31.
[10] L. Wang, J. Zhang, R. Zhao, Y. Li, C. Li, C. Zhang, Adsorption of Pb (II) on activated carbon prepared from Polygonum orientale Linn.: Kinetics, isotherms, pH, and ionic strength studies, Bioresour. Technol. 101 (2010) 5808–5814.
[11] R. Zein, R. Suhaili, F. Earnestly, E. Munaf, Removal of Pb(II), Cd(II) and Co(II) from aqueous solution using Garcinia mangostana L. fruit shell, J. Hazard. Mater. 181 (2010) 52–56.
[12] E.S.Z. El-Ashtoukhy, N. Amin, O. Abdelwahab, Removal of lead (II) and copper (II) from aqueous solution using pomegranate peel as a new adsorbent, Desalination 223 (2008) 162–173.
[13] H. Zhang, Y. Yan, L. Yang, Preparation of activated carbon from sawdust by zinc chloride activation, Adsorption 16 (2010) 161–166.

[14] T.M. Alslaibi, I. Abustan, M.A. Ahmad, A. Abu Foul, Effect of different olive stone particle size on the yield and surface area of activated carbon production, Adv. Mater. Res. 626 (2013) 126–130.
[15] T.M. Alslaibi, I. Abustan, M.A. Ahmad, A. Abu Foul, Preparation of activated carbon from olive stone waste: Optimization study on the removal of Cu^{2+}, Cd^{2+}, Ni^{2+}, Pb^{2+}, Fe^{2+} and Zn^{2+} from aqueous solution using response surface methodology, J. Dispersion Sci. Technol. (2013), doi: 10.1080/01932691.2013.809506.
[16] M.A. Bezerra, R.E. Santelli, E.P. Oliveira, L.S. Villar, L.A. Escaleira, Response surface methodology (RSM) as a tool for optimization in analytical chemistry, Talanta 76 (2008) 965–977.
[17] M.J.K. Bashir, H.A. Aziz, M.S. Yusoff, S.Q. Aziz, Color and chemical oxygen demand removal from mature semi-aerobic landfill leachate using anion-exchange resin: An equilibrium and kinetic study, Environ. Eng. Sci. 29 (2012) 297–305.
[18] N. Fiol, I. Villaescusa, M. Martínez, N. Miralles, J. Poch, J. Serarols, Sorption of Pb(II), Ni(II), Cu(II) and Cd(II) from aqueous solution by olive stone waste, Sep. Purif. Technol. 50 (2006) 132–140.
[19] W. Ngah, S. Ab Ghani, A. Kamari, Adsorption behaviour of Fe (II) and Fe (III) ions in aqueous solution on chitosan and cross-linked chitosan beads, Bioresour. Technol. 96 (2005) 443–450.
[20] A. Iup, Manual of symbols and terminology for physicochemical quantities and units, Appendix II, Part I, definitions, terminology and symbols in colloid and surface chemistry, Pure Appl. Chem. 31 (1972) 579–638.
[21] M.A. Ahmad, R. Alrozi, Removal of malachite green dye from aqueous solution using rambutan peel-based activated carbon: Equilibrium, kinetic and thermodynamic studies, Chem. Eng. J. 171 (2011) 510–516.
[22] J. Yang, K. Qiu, Preparation of activated carbons from walnut shells via vacuum chemical activation and their application for methylene blue removal, Chem. Eng. J. 165 (2010) 209–217.
[23] N.H. Phan, S. Rio, C. Faur, L. Le Coq, P. Le Cloirec, T.H. Nguyen, Production of fibrous activated carbons from natural cellulose (jute, coconut) fibers for water treatment applications, Carbon 44 (2006) 2569–2577.
[24] A. Ahmad, B. Hameed, Effect of preparation conditions of activated carbon from bamboo waste for real textile wastewater, J. Hazard. Mater. 173 (2010) 487–493.
[25] A.B. Pérez-Marín, V.M. Zapata, J.F. Ortuño, M. Aguilar, J. Sáez, M. Lloréns, Removal of cadmium from aqueous solutions by adsorption onto orange waste, J. Hazard. Mater. 139 (2007) 122–131.
[26] R. Sitko, B. Zawisza, E. Malicka, Modification of carbon nanotubes for preconcentration, separation and determination of trace-metal ions, TrAC, Trends Anal. Chem. 37 (2012) 22–31.
[27] R. Han, P. Han, Z. Cai, Z. Zhao, M. Tang, Kinetics and isotherms of Neutral Red adsorption on peanut husk, J. Environ. Sci. 20 (2008) 1035–1041.
[28] B. Hameed, M. El-Khaiary, Equilibrium, kinetics and mechanism of malachite green adsorption on activated carbon prepared from bamboo by K_2CO_3 activation and subsequent gasification with CO_2, J. Hazard. Mater. 157 (2008) 344–351.
[29] M. Chabani, A. Amrane, A. Bensmaili, Kinetics of nitrates adsorption on Amberlite IRA 400 resin, Desalination 206 (2007) 560–567.
[30] S. Ho Lee, C. Hun Jung, H. Chung, M. Yeal Lee, J.W. Yang, Removal of heavy metals from aqueous solution by apple residues, Process Biochem. 33 (1998) 205–211.
[31] D. Božić, V. Stanković, M. Gorgievski, G. Bogdanović, R. Kovačević, Adsorption of heavy metal ions by sawdust of deciduous trees, J. Hazard. Mater. 171 (2009) 684–692.
[32] L. Mouni, D. Merabet, A. Bouzaza, L. Belkhiri, Adsorption of Pb(II) from aqueous solutions using activated carbon developed from Apricot stone, Desalination 276 (2011) 148–153.
[33] T.M. Alslaibi, I. Abustan, M.A. Ahmad, A. Abu Foul, Application of response surface methodology (RSM) for optimization of Cu^{2+}, Cd^{2+}, Ni^{2+}, Pb^{2+}, Fe^{2+}, and Zn^{2+} removal from aqueous solution using microwaved olive stone activated carbon, J. Chem. Technol. Biotechnol. (2013), doi: 10.1002/jctb.4073.
[34] B. Acemioğlu, Removal of Fe (II) ions from aqueous solution by Calabrian pine bark wastes, Bioresour. Technol. 93 (2004) 99–102.
[35] L. Agouborde, R. Navia, Heavy metals retention capacity of a non-conventional sorbent developed from a mixture of industrial and agricultural wastes, J. Hazard. Mater. 167 (2009) 536–544.
[36] S. Shukla, R.S. Pai, Adsorption of Cu (II), Ni (II) and Zn (II) on modified jute fibres, Bioresour. Technol. 96 (2005) 1430–1438.
[37] U. Saha, S. Taniguchi, K. Sakurai, Simultaneous adsorption of cadmium, zinc, and lead on hydroxyaluminum-and hydroxyaluminosilicate-montmorillonite complexes, Soil Sci. Soc. Am. J. 66 (2002) 117–128.
[38] H.A. Aziz, M.S. Yusoff, M.N. Adlan, N.H. Adnan, S. Alias, Physico-chemical removal of iron from semi-aerobic landfill leachate by limestone filter, Waste Manage. 24 (2004) 353–358.
[39] I. Tan, A. Ahmad, B. Hameed, Optimization of preparation conditions for activated carbons from coconut husk using response surface methodology, Chem. Eng. J. 137 (2008) 462–470.
[40] Q. Li, J. Zhai, W. Zhang, M. Wang, J. Zhou, Kinetic studies of adsorption of Pb (II), Cr (III) and Cu (II) from aqueous solution by sawdust and modified peanut husk, J. Hazard. Mater. 141 (2007) 163–167.
[41] P. Brown, I. Atly Jefcoat, D. Parrish, S. Gill, E. Graham, Evaluation of the adsorptive capacity of peanut hull pellets for heavy metals in solution, Adv. Environ. Res. 4 (2000) 19–29.
[42] M. Spinti, H. Zhuang, E.M. Trujillo, Evaluation of immobilized biomass beads for removing heavy metals from wastewaters, Water Environ. Res. 67 (1995) 943–952.
[43] S. Tangjuank, N. Insuk, J. Tontrakoon, V. Udeye, Adsorption of lead (II) and cadmium (II) ions from aqueous solutions by adsorption on activated carbon prepared from cashew nut shells, World Academy Sci.: Eng. Technol. 52 (2009) 110–116.
[44] S. Shukla, R.S. Pai, A.D. Shendarkar, Adsorption of Ni (II), Zn (II) and Fe (II) on modified coir fibres, Sep. Purif. Technol. 47 (2006) 141–147.
[45] V.K. Gupta, C. Jain, I. Ali, M. Sharma, V. Saini, Removal of cadmium and nickel from wastewater using bagasse fly ash-a sugar industry waste, Water Res. 37 (2003) 4038–4044.
[46] B. Bayat, Comparative study of adsorption properties of Turkish fly ashes: I. The case of nickel (II), copper (II) and zinc (II), J. Hazard. Mater. 95 (2002) 251–273.
[47] Y. Ho, D. Wase, C. Forster, Kinetic studies of competitive heavy metal adsorption by sphagnum moss peat, Environ. Technol. 17 (1996) 71–77.
[48] M. Iqbal, A. Saeed, N. Akhtar, Petiolar felt-sheath of palm: A new biosorbent for the removal of heavy metals from contaminated water, Bioresour. Technol. 81 (2002) 151–153.
[49] S. Shukla, R.S. Pai, Adsorption of Cu (II), Ni (II) and Zn (II) on dye loaded groundnut shells and sawdust, Sep. Purif. Technol. 43 (2005) 1–8.
[50] H. Qiu, L. Lv, B. Pan, Q. Zhang, W. Zhang, Critical review in adsorption kinetic models, J. Zhejiang Univer.-Sci. A 10 (2009) 716–724.
[51] B. Hameed, Spent tea leaves: A new non-conventional and low-cost adsorbent for removal of basic dye from aqueous solutions, J. Hazard. Mater. 161 (2009) 753–759.